Hindawi
Shock and Vibration
Volume 2023, Article ID 9707114, 19 pages
https://doi.org/10.1155/2023/9707114

Research Article

Study on the Safety Evaluation Method of Life-Saving Passage in Building Ruins under the Action of Aftershock

Xu Defeng,[1] Dai Junwu,[2,3] Chen Limei,[1] Yang Yongqiang,[2,3] and Richard Agyare[4]

[1]*Jilin Agricultural University, Changchun 131118, China*
[2]*Institute of Engineering Mechanics of China Earthquake Administration, Harbin 150080, China*
[3]*Key Laboratory of Earthquake Engineering and Engineering Vibration of China Earthquake Administration, Harbin 150080, China*
[4]*College of Civil Engineering, Tongji University, Shanghai 200092, China*

Correspondence should be addressed to Chen Limei; chenlmm@163.com

Received 16 August 2022; Revised 25 February 2023; Accepted 4 March 2023; Published 15 April 2023

Academic Editor: Moustafa Moufid Kassem

It is essential to evaluate the safety of the life-saving passage in building ruins and to ensure the "double safety" of rescuers and trapped people during the earthquake rescue; however, there are few studies on the safety evaluation method of life-saving passage. In this paper, the vertical displacement of wood shoring is proposed as an evaluation indicator of the saving-life passage considering the characteristics of building ruins and the size of the living space of the trapped. Taking life-saving passage of the pancake-type building ruins as research object, the evaluation of the safety of the life-saving passage was investigated under the action of aftershock. The vertical bearing capacity test of wood shoring is performed in order to obtain the evaluation indicator of saving-life passage. The restart function of ANSYS/LS-DYNA program is used to re-edit the numerical model of the building ruins to construct the life-saving passage, then, the safety evaluation of life-saving passage of the pancake-type building ruins is investigated under the action of aftershock. The results show that the constructed life-saving passage passed the safety evaluation under the actions of different aftershocks. The possibility of the secondary collapse of the life-saving passage increases exponentially with the increase of rescue time within "72-hour gold rescue," and the growth is slow after 72 hours when the magnitude of the main earthquake reaches above 7.4; the safety factor K should be increased appropriately if wood shoring is used to construct a life-saving passage when the main earthquake's magnitude is greater than or equal to 7.5. The safety evaluation method of life-saving passage can provide effective reference for earthquake rescue.

1. Introduction

Not only are the trapped people in danger during the earthquake emergency rescue process but also the rescuers. Over 100 rescuers and volunteers died due to the secondary collapse of building ruins during the rescue process in the 1985 Mexico City 8.1 magnitude earthquake (Xu) [1]. Several rescuers were injured and killed due to the rescue in the 2008 China Wenchuan magnitude 8.0 earthquake (Chen) [2]. A large number of rescue workers and trapped people died in earthquake rescue according to a systematic review of OR and MS research in humanitarian operations [3, 4]. Rescuers and volunteers are often injured and killed due to the secondary collapse of the building ruins, which caused the construction of life-saving passage [5]. Therefore, evaluating the safety of the life-saving passage in building ruins is important to ensure the "double safety" of rescuers and trapped people in the earthquake rescue process. Currently, the safety evaluation of life-saving passage at earthquake rescue sites both domestically and internationally is mainly based on the professional and technical capabilities of Specialized Search and Rescue (SAR) team and Search and Rescue Guidelines (SAG) [6]. In 1998, the United States released the "Field operation guideline" (U.S. Army Corps of Engineers) [7], which gives the methods and steps of the safety evaluation of the life-saving passage in building ruins.

Furthermore, in 2002, the United Nations Search and Rescue Advisory Group formulated the International Search and Rescue Guide (INSARAG) [8] to clarify the safety evaluation steps, including the building ruins' rapid evaluation method, the structural engineer's evaluation of the group building at the rescue site, the hazardous substances at the rescue site, and rescue subtree strategies and procedures for constructing the life-saving passage in building ruins. In 2001, the National Earthquake Rescue Team, also known as China International Search and Rescue (CISAR) [9], was established to evaluate the safety of building ruins at earthquake rescue sites in China. Meanwhile, USAR has undertaken earthquake emergency rescue work due to the establishment of USAR team in some countries. For example, the 1986 Kalamata earthquake struck the southern Peloponnese of Greece on September 13 at 20:24 local time [10]. The rescuers of USAR immediately participated in the emergency rescue of two buildings ruins in Kalamata. Rescuers took 6-7 hours to adopt the horizontal penetration in order to contact with a trapped person located 3-4 m away from the facade [11]. In the 1999 Ji-Ji Earthquake in Taiwan, China, 309 rescuers of USAR have been assigned to the site of the collapsed building. As to the collapsed Dong-Xing building that buried 100 people, the rescuers of USAR carried out rescue work based on the rescue standards and guidelines. After 7 days, only 27 people were rescued [12]. In the 2008 China Wenchuan Ms 8.0 earthquake rescue process, the rescuers of China USAR carried out rescue work on a hotel building that buried 10 people. There are several aftershocks during the rescue process. The rescuers adopted the conservative layer stripping method to carry out this rescue according to "INSARAG." Although 5 people were rescued after 3 days, the rescue speed was still slowed down [13]. According to the abovementioned rescue cases, USAR is particularly time-consuming and technically demanding because operations are spread over very large, often densely populated areas, with structural complications related to the interlocking of buildings in older and most vulnerable city centers. To this end, Hitomi MURAKAMI analyzed 1900 search and rescue cases of the 1995 Hanshin-Awaji earthquake, which illustrated that the success rate of earthquake emergency rescue is closely related to USAR professional equipment, technical capabilities, and safety evaluation experiences [14]. Koresawa analyzed the search and rescue operations following the great east Japan earthquake, which demonstrated the rescuers of USAR lacked experience in safety assessment of building ruins and effective rescue equipment [15]. The 2023 Turkey 7.8 Ms earthquake has directly caused 42310 deaths. USAR teams from 66 countries have arrived in Turkey to carry out rescue work [16]. There were many strong aftershocks, which caused great difficulties for earthquake rescue. Meanwhile, it was snowing, which caused a great threat to the trapped people under the building ruins. Although rescuers from various countries have rescued many survivors, many trapped people have not been rescued. Thus, the scientific and effective safety assessment of building ruins still poses a challenge to the rescue due to the poor rescue environment [17]. On the whole, USAR in many countries has established corresponding earthquake rescue standards and guidelines. However, there is still room for improvement, especially, the safety evaluation methods in the above rescue standards and guidelines of USAR are primarily based on the experience of seismic rescue and structural engineering experts. Therefore, the theoretical studies on the safety evaluation of life-saving passages in building ruins to improve the earthquake rescue efficiency are essential.

Presently, researchers, both domestically and internationally, mainly focus on safety evaluation management and the expert system construction of building ruins. For instance, in 2013, Wang [18] highlighted that most building ruins are temporarily stable and that various possible situations may cause the building ruins' instability during the rescue process. Thus, preventive measures should be taken, and a comprehensive management system for the safety evaluation of building ruins has been established. In 2015, Liu [19] launched research on the expert system for the safety evaluation of building ruins, completed the preliminary design of the expert system of safety evaluation, and demonstrated the safety evaluation of building ruins in the actual rescue case. To evaluate the safety of building ruins, seismic rescue experts in China usually refer to "Dangerous Building Appraisal Standards" (JGJ125-99 2004) [20] and "Earthquake Site Work Part II: Building Safety Appraisal" (GB18208.2 2001) [21]. Additionally, a systematic review of prediction methods for emergency management and seismic vulnerability assessment methodologies were published [22, 23]. However, the above standards only divide the damage level of collapsed buildings, but the impact factors of the construction of life-saving passages in building ruins are not considered, for example, the influence of aftershocks on the safety of the life-saving passages. It is widely known that the biggest safety hazard is the aftershock at the earthquake rescue site [24]. The main reason is that the arrival time of the aftershock cannot be predicted, causing rescuers to always face the threat of aftershock when they enter the building ruins to rescue trapped people. Simultaneously, rescue techniques (such as shoring, removal, and demolition) are usually used to construct life-saving passages in building ruins as safety paths [25, 26]. Thus, the safety evaluation of life-saving passages is particularly important, which is one of the critical factors for the success or failure of an earthquake emergency rescue. The different approaches, such as earthquake rescue site, the virtual ruins scenes, need to be elaborated in order to evaluate the safety of life-saving passage in building ruins. The safety of life-saving passage at the seismic rescue site is usually evaluated according to relevant specifications and experience of rescue experts. Simultaneously, there are few relevant on-site records and literature due to the emergency rescue time at the earthquake site. The virtual scenes of building ruins have been constructed at home and abroad to improve the rescue ability and enhance rescue experience of rescue teams. For example, Miami Emergency Rescue Center of the United States spent 400 million dollars to build a simulation training building ruins [27]. The Russian "179" training base set up a scene of building ruins of urban search and rescue training with a total investment of $15. In 1999, a simulation training scene of earthquake ruins was built in the Singapore

Civil Defense Academy of Civil Buildings [28]. In 2000, four typical building ruins were built in USAR training center in China, such as, pancake-type building ruins, incline-type building ruins, small space-type building ruins, and V-type building ruins [29]. The rescue trainers can construct and evaluate the life-saving passage in the abovementioned building ruins by observing the displacement changes of the key measuring points in the building ruins [30]. However, the virtual ruins scenes have many problems, such as high cost, small quantity, single form, etc., which leads to the ineffective and adequate implementation of training drills for the construction and evaluation of life-saving passage. The method of numerical simulation is currently adopted to solve strongly nonlinear dynamic response problem, which involves to the simulation of building collapse and ruins under the action of earthquake [31–33]. However, the numerical simulation method of life-saving passage in building ruins is rarely studied by researchers. The reason is that few investigators pay attention to the secondary collapse of building ruins, additionally, the dynamic response analysis of building ruins under the aftershock is and also a difficulty. However, some finite element software can provide restart analysis to solve the abovementioned problem, for example, the full-restart fiction of LS-DYNA program [34]. The construction and evaluation of life-saving passage in building ruins cannot be separated from rescue technology including the removal, shoring, uplift, and breach rescue technology according to "INSARAG International Search and Rescue Guide" [8]. Specially, shoring rescue technology can protect building ruins from secondary collapse to a certain extent during the process of construction of life-saving passage [35–37]. In addition, the safety assessment of the life-saving passage is realized through the early warning of the crack change of the wood shoring, the crushing of surface, the abnormal sound, etc. [38–40]. Currently, the numerical simulation of using shoring technology to construct life-saving passage has hardly been investigated. Moreover, there is a lack of the bearing capacity test of wood shoring in China. In summary, theoretical studies on the safety evaluation of life-saving passage in building debris remain underexplored locally and internationally. Hence, this paper aims to study the safety evaluation of life-saving passages using numerical simulation method, considering the needs of the earthquake rescue process.

The main purpose of the safety evaluation of the life-saving passages in building ruins is to evaluate whether secondary collapse will happen to the life-saving passage under the action of aftershocks. Thus, studies on obtaining the evaluation indicator and the numerical simulation method for the secondary collapse of the life-saving passage are imperative. Subsequently, a reasonable and scientific evaluation indicator of the secondary collapse of life-saving passages will be discussed in Section 2. In Section 3, the safety evaluation method under aftershocks is studied using the pancake's building ruins as the research objective. In Section 4, the possibility of the secondary collapse of life-saving passages under the actions of aftershocks after the main earthquake will be analyzed.

2. The Safety Evaluation Indicator

The safety evaluation indicator of the life-saving passages in building ruins can be selected by referring to the structural seismic damage indicator, the domestic and foreign building structural seismic design codes, and the monitoring indicator of the damaged structure. Among these, the structural seismic damage indicator is used to evaluate the whole process of the structure from damage to collapse under an earthquake. For instance, Allahabadi and Powell [41] proposed an improved ductility ratio as a structural damage evaluation, and deformation beyond the elastic limit is the leading cause of structural failure. Banon et al. [42] proposed deformation accumulation as a safety evaluation indicator. Gosain et al. [43] used the energy method to evaluate structural damage and gave a simple formula for calculating the cumulative ratio. Park et al. [44] proposed a damage classification method divided into damage characteristics corresponding to no damage, slight damage, moderate damage, severe damage, and collapsed states. Roufauel and Meyer [45] established a simple relationship between the overall damage parameter expressed by the top deformation and the corresponding fundamental frequency change by structural modal parameters. The abovementioned structural seismic damage indicators can be used to evaluate different degrees of damage. However, obtaining the above seismic damage parameters is difficult due to the strong nonlinear and discrete discontinuous characteristics of the building ruins material. The structure damage limit values are also given in the domestic and foreign building structure design codes; for example, the Tall Buildings Initiative (TBI)—Guidelines for Performance-Based Seismic Design of Tall Buildings—in the US [46] gives the peak transient story drift ratio as the criterion of structural collapse. In addition, the "Code for Seismic Design of Building" (GB50011–2010) in China [47] gives the limit values of the elastic and plastic story drift ratio. The "Standard for Anticollapse Design of Building Structures" (T/CECS 392-2021) [48] stipulates that the structure is considered to collapse if the vertical deformation of the structure affects the safe usage spaces of the structure. Studies on safety evaluation and early warning of damaged structures by scholars domestically and abroad have established certain reference values for the safety evaluation of life-saving passages in building ruins. For instance, Nicola [49] utilized monitoring equipment to predict landslides and used the displacement and velocity time history of monitoring points as safety discriminant indicators to complete early warnings of landslides. Pratesi et al. [50] monitored the inclination of the ancient Italian city wall caused by the earthquake and completed a safety evaluation and early warning of the city wall by monitoring the structural displacement and velocity time history response of the wall.

A suitable and scientific safety evaluation indicator of life-saving passages in building ruins is proposed to consider two factors: the structural characteristics of building ruins and the trapped people affected by the survival space in building ruins. Building ruins are prone to vertical displacement under aftershocks due to the nonlinear damage characteristics of

structural ruin material, and trapped people are greatly affected by vertical space. Simultaneously, it is feasible to use vertical displacement as the evaluation indicator by referring to the "Standard for Anticollapse Design of Building Structures" and the safety monitoring and early warning of damaged structures. Therefore, vertical displacement was selected as the safety evaluation indicator of life-saving passages in building ruins. This paper considers wood shoring as a necessary rescue technology for constructing a life-saving passage in building ruins. For example, a 9-storey federal building exploded in Oklahoma City on April 19, 1995 [51]. Wood shoring was placed on the first floor to prevent the building from collapsing again, which directly impacted the stability and safety of the life-saving passage, as shown in Figure 1. Therefore, the safety of the life-saving passages can be measured by the vertical deformation of the wood shoring. Hence, it is necessary to determine the vertical deformation capacity of wood shoring using the bearing capacity test. It is considered unsafe if the vertical deformation (D) of the life-saving passages exceeds the allowable deformation value (or discrimination limit $[D]$) of the wood shoring itself under the actions of aftershocks. Conversely, it is safe, as expressed in formulas (1) and (2).

$$D < [D], \text{safe}, \tag{1}$$

$$D \geq [D], \text{unsafe}. \tag{2}$$

Eighteen double columns (DC) and nine three-dimensional (3D) vertical bearing capacity tests of wood shoring were designed and completed to obtain the vertical displacement value. The loading device uses a servo-hydraulic testing machine with a loading capacity of 50 tons and a displacement range of ±300 mm. Figures 2–5 show the loading device and calculation diagram. The loading method of the wood shoring test refers to the "Standard for Method Testing of Timber Structures" (GB/T 50329-2012) [52], and displacement-controlled loading is adopted with a speed of 0.05 mm/s until the wood shoring fails completely. The compressive ultimate bearing capacity (UBC) and ultimate vertical deformation of DC and 3D wood shoring and mean value are shown in Table 1. The relationship between D_{ultimate} and H of DC and 3D wood shoring is given, where D_{ultimate} is the ultimate vertical deformation of wood shoring, and H is the column height of wood shoring, as shown in Figures 6 and 7.

Table 1 shows the BC and D values of the wood shoring. The design value is expected to be used in the actual rescue process. The allowable stress design method is used to determine the design value, and the relationship between the design value (F_d) and the ultimate bearing capacity (F_u) is established, as expressed in formulas (3) and (4).

$$F_d = \frac{F_u}{K}, \tag{3}$$

$$K = C_d \times C_p, \tag{4}$$

where K is the safety coefficient of wood shoring, C_d is the loading duration factor, and C_p is the influence coefficient considering the rescuer's psychological factors. C_d is

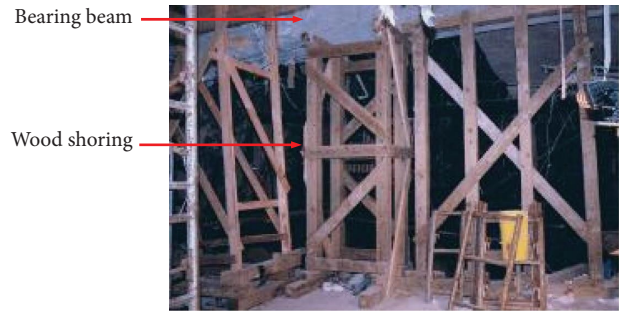

Figure 1: Application scenario of wood shoring in Murrah Federal building (O'Connell [52]).

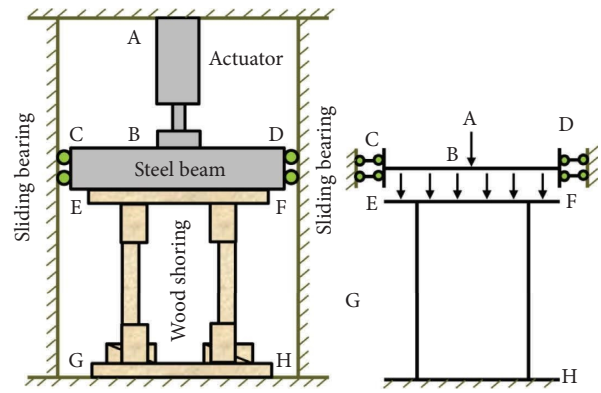

Figure 2: Schematic diagram of the loading device of the axial compression test of DC wood shoring.

determined by referring to the national design specification for wood construction in the US [53], and the value of C_d is 1.6, as shown in Table 2.

The test found that wood shoring makes a dense sound when the deformation of the wood shoring wedge increases, which causes serious psychological pressure on the rescuers. The wood shoring wedge makes some dense noise when the deformation curve reaches point B by recording the test phenomena. Thus, point B is taken as the compressive bearing capacity in the actual earthquake rescue, and the ratio of F_B to the ultimate bearing capacity (F_u) as the influence coefficient C_p, that is, $C_p = F_u/F_B$. Through the statistical analysis, the relationship between F_B of wood shoring point B and F_u is shown in Figures 8 and 9, and the following is obtained, $C_p = 1.96–2.32$, and $K = C_d \times C_p = 1.6 \times (1.43\sim1.68) = 2.3–2.7$.

The allowable stress design is used to determine that the safety factor K of wood shoring is 2.5, and the bearing capacity of the design value is equal to the ultimate bearing capacity divided by 2.5.

First, the type and size of the wood shoring were determined to construct the life-saving passages in building ruins, then, the ultimate vertical displacement (D_{ultimate}) of the wood shoring was determined, as shown in Figures 6 and 7, and the allowable deformation value of the wood shoring itself $[D]$ is determined according to the safety factor K of the wood shoring. Finally, the discrimination limit of the secondary collapse of the life-saving passages in building ruins is obtained, as shown in formula.

Figure 3: The test device of DC wood shoring.

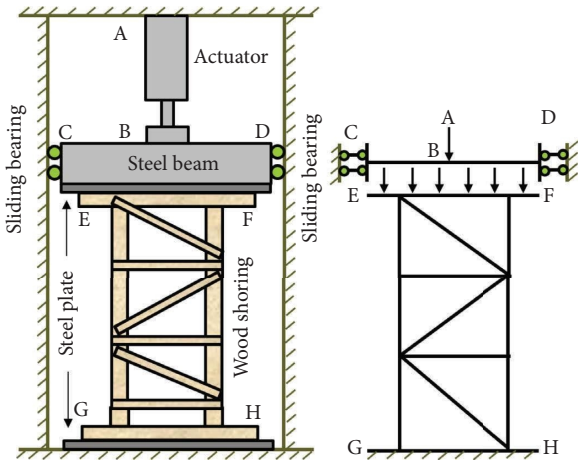

Figure 4: Schematic diagram of the loading device of the axial compression test of 3D wood shoring.

Figure 5: The test device of 3D wood shoring.

$$[D] = \frac{D_{\text{ultimate}}}{2.5}. \tag{5}$$

Table 1: Ultimate bearing capacity, deformation, and mean value of wood shoring deformation (bearing capacity unit: kN; deformation unit: mm).

No.	*Type*	*DC-1*	*DC-2*	*DC-3*	*DC-4*	*DC-5*	*DC-6*
Specimen-1	UBC	280.4	228.0	191.9	158.5	128.8	92.8
	D_{ultimate}	168.1	156.5	144.8	126.4	100.2	86.2
Specimen-2	UBC	311.5	276.8	235.5	173.1	134.4	105.3
	D_{ultimate}	188.2	175.2	159.8	138.9	112.4	79.5
Specimen-3	UBC	229.5	241.0	241.0	242.4	136.3	101.7
	D_{ultimate}	171.2	178.3	149.5	150.2	110.2	88.5
Mean value	BC	269.8	248.6	222.8	191.3	133.2	99.9
	D_{ultimate}	175.8	170.0	151.4	138.5	107.6	84.7
No.	*Type*	*3D-1*	—	*3D-2*	—	*3D-3*	—
Specimen-1	UBC	399.5	—	370.7	—	355.2	—
	D_{ultimate}	189.6	—	178.2	—	170.6	—
Specimen-2	UBC	435.3	—	350.7	—	372.5	—
	D_{ultimate}	200.3	—	181.3	—	188.2	—
Specimen-3	UBC	367.7	—	407.0	—	328.5	—
	D_{ultimate}	185.2	—	197.5	—	152.3	—
Mean value	UBC	401.5	—	376.1	—	352.1	—
	D_{ultimate}	191.7	—	185.7	—	170.4	—

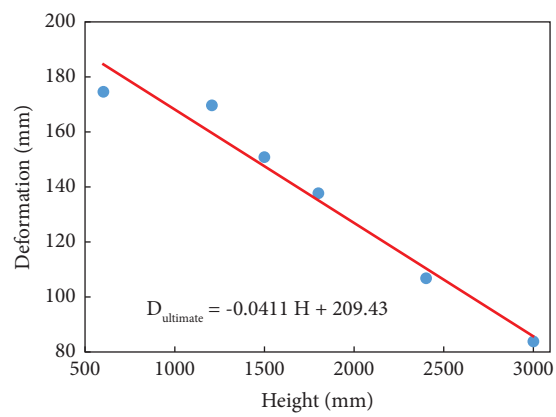

Figure 6: Relationship between D_{ultimate} and H of DC wood shoring.

3. The Safety Evaluation of Life-Saving Passage under Aftershock

The selection of aftershocks and their magnitudes is crucial for the safety evaluation of life-saving passages. Thus, the probability percentage (P_i) of each aftershock magnitude within 168 hours after the main earthquake 8.0 is counted. The main aftershocks statistical data include the 1966–2002 China Earthquake Examples [54], 2003–2021 Official Website of the U.S. Geological Survey [55]. The statistical method is not described in detail, but the statistical results are given in Table 3. First, the building ruins in the 2008 China Wenchuan magnitude 8.0 earthquake were selected as the research objects. Then, the life-saving passage was constructed through corresponding rescue technology, especially shoring technology. Finally, the safety of the life-

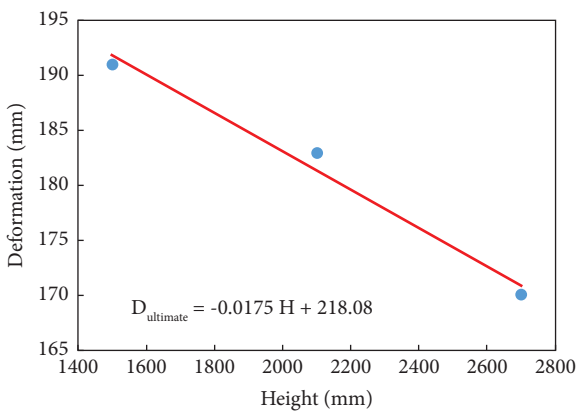

Figure 7: Relationship between D_{ultimate} and H of 3D wood shoring.

Table 2: Frequently used load duration factors C_d.

Load duration	C_d	Typical design loads
Permanent	0.9	Dead load
Ten years	1.0	Occupancy live load
Two mouths	1.15	Snow load
Seven days	1.25	Construction load
Ten minutes	1.6	Wind/earthquake load
Impact	2.0	Impact load

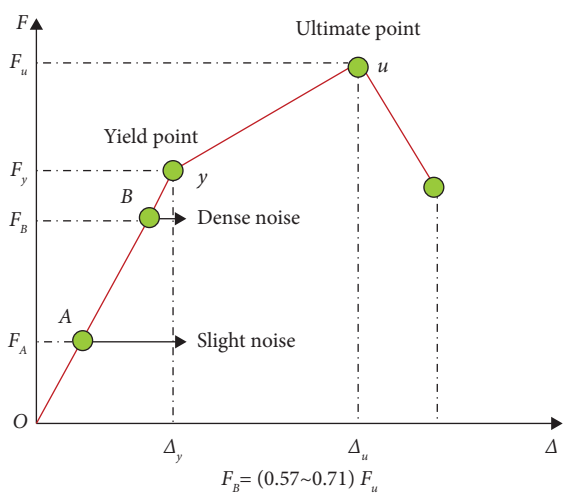

Figure 8: The whole process of DC failure.

saving passage was evaluated. According to Table 3, the aftershock magnitude with the greatest possibility of a magnitude 8.0 earthquake is Ms 4.0–4.4, and the maximum aftershock magnitude is Ms 6.4 as the evaluation magnitude. The actual earthquake rescue [56–58] shows that the survival rate of the trapped people within the "golden rescue 72 hours" is high. Meanwhile, many destructive earthquakes have proved the importance of rescue within 72 hours. However, there is still a certain chance of survival 72 hours after the earthquake. For example, in 2008 China Wenchuan Ms 8.0 earthquake, hundreds of trapped people were still rescued from the building ruins after the golden rescue

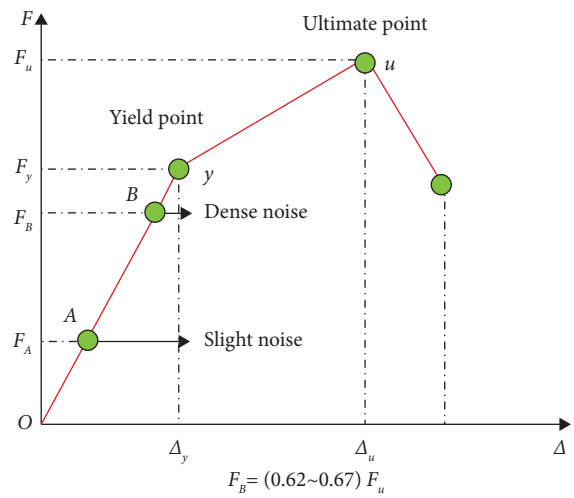

Figure 9: The whole process of 3D failure.

72 hours [59]. In 2023 Turkey earthquake rescue, a 7-month-old baby was rescued 136 hours after the earthquake [60], and some trapped people were successfully rescued 150 hours after the earthquake [61]. There are many similar examples in Turkey earthquake rescue. Therefore, this paper not only considers the aftershock record statistics of golden rescue 72 hours but also 72–168 hours. The selection of aftershocks considers two factors: the near field and the location of the building ruins. Therefore, 28 classical near-field ground motion records in FEMA695 Appendix A [62] and 28 Wenchuan aftershocks [63] were selected, as shown in Tables 4 and 5.

The safety evaluation of the life-saving passage was conducted by inputting aftershock magnitudes of 4.4 and 6.4 ground motions. The relationship between aftershock magnitude and peak ground acceleration (PGA) was established to simplify the calculation because the magnitudes of ground motion are different in Tables 4 and 5. The approximate PGA values corresponding to different magnitudes within 10 km in the near field were obtained according to the PGA attenuation relationship curve given by Boore and Atkinson [64] and Jiang [65], as shown in Table 6. The PGA of different aftershocks was normalized, and then the amplitude was modulated to 0.06 g and 0.35 g.

The author used LS-DYNA software to simulate the seismic collapse of the reinforced concrete frame structure of Xuankou middle school in Beichuan County during the 2008 Wenchuan earthquake, and the building ruins in the form of pancake type (Xu et al.) [66], as shown in Figure 10. A 3D wood shoring with a height of 2.1 meters was added to the axes 15 of the key damage position in the building ruins, and the discrimination limit of vertical displacement of secondary collapse $[D] = 73.2$ mm was obtained according to Figure 7 and formula (5). Supposing there are trapped people between axis 10 and 11, the section of building ruins is obtained by cutting along axis 1-1 and taking axis 10–15, as shown in Figure 11. The restart analysis method of LS-DYNA software was used to change the acceleration time history curve of the original numerical model of building

Table 3: Probability percentage (P_i) of aftershock magnitude occurrence after different main shock magnitudes within 168 hour (H).

Main earthquake magnitude	Statistical interval (H)	Aftershock magnitude							
		4.0–4.4 (%)	4.5–4.9 (%)	5.0–5.4 (%)	5.5–5.9 (%)	6.0–6.4 (%)	6.5–6.9 (%)	7.0–7.4 (%)	≥7.5
6.0–6.4	≤12	53.19	21.28	25.53	6.38	2.13			
	≤24	55.32	27.66	29.79	10.64	2.13			
	≤48	55.32	34.04	34.04	12.77	4.26			
	≤72	55.32	38.30	34.04	14.89	4.26			
	≤96	55.32	38.30	34.04	14.89	4.26			
	≤120	55.32	40.43	34.04	14.89	6.38			
	≤144	59.57	40.43	36.17	14.89	6.38			
	≤168	59.57	42.55	36.17	17.02	6.38			
6.5–6.9	≤12	89.29	67.86	21.43	21.43				
	≤24	89.29	67.86	35.71	25.00				
	≤48	92.86	71.43	35.71	28.57				
	≤72	92.86	71.43	42.86	28.57				
	≤96	92.86	71.43	42.86	28.57	3.57			
	≤120	92.86	82.14	42.86	28.57	3.57			
	≤144	92.86	85.71	46.43	28.57	3.57			
	≤168	92.86	85.71	46.43	28.57	3.57			
7.0–7.4	≤12	100.00	78.57	64.29	35.71	7.14	7.14		
	≤24	100.00	85.71	64.29	35.71	7.14	7.14		
	≤48	100.00	85.71	71.43	35.71	14.29	14.29		
	≤72	100.00	85.71	71.43	50.00	21.43	14.29		
	≤96	100.00	85.71	85.71	50.00	21.43	14.29		
	≤120	100.00	85.71	85.71	50.00	21.43	14.29		
	≤144	100.00	85.71	85.71	50.00	21.43	21.43		
	≤168	100.00	85.71	85.71	50.00	21.43	21.43	7.14	
≥7.5	≤12	100.00	85.71	71.43	42.86	28.57	14.29	14.29	
	≤24	100.00	85.71	85.71	57.14	28.57	28.57	28.57	
	≤48	100.00	85.71	85.71	57.14	42.86	28.57	28.57	
	≤72	100.00	85.71	85.71	57.14	42.86	28.57	42.86	
	≤96	100.00	85.71	85.71	57.14	42.86	28.57	42.86	
	≤120	100.00	85.71	85.71	57.14	42.86	28.57	42.86	
	≤144	100.00	85.71	85.71	57.14	42.86	28.57	42.86	
	≤168	100.00	85.71	85.71	57.14	42.86	28.57	42.86	

Table 4: 28 near-field ground motion records in FEMA P695 Appendix A.

No.	Magnitude (Ms)	Year	PGA (g)	Earthquake	Recording station	
				Name	Name	Owner
1	6.5	1979	0.44	Imperial valley-06	El Centro array #6	CDMG
2	6.5	1979	0.46	Imperial valley-06	El Centro array #7	USGS
3	6.9	1980	0.31	Irpinia, Italy-01	Sturno	ENEL
4	6.5	1987	0.642	Superstition hills-02	Parachute test site	USGS
5	6.9	1989	0.38	Loma prieta	Saratoga-Aloha	CDMG
6	6.7	1992	0.49	Erzican, Turkey	Erzincan	—
7	7	1992	0.63	Cape Mendocino	Petrolia	CDMG
8	7.3	1992	0.79	Landers	Lucerne	SCE
9	6.7	1994	0.87	Northridge-01	Rinaldi receiving sta.	DWP
10	6.7	1994	0.73	Northridge-01	Sylmar-olive view	CDMG
11	7.5	1999	0.22	Kocaeli, Turkey	Izmit	ERD
12	7.6	1999	0.82	Chi-Chi, Taiwan	TCU065	CWB
13	7.6	1999	0.29	Chi-Chi, Taiwan	TCU102	CWB
14	7.1	1999	0.52	Duzce, Turkey	Duzce	ERD
15	6.8	6.8	0.71	Gazli, USSR	Karakyr	—
16	6.5	1979	0.76	Imperial valley-06	Bonds corner	USGS
17	6.5	1979	0.28	Imperial valley-06	Chihuahua	UNAMUCSD
18	6.8	1985	1.18	Nahanni, Canada	Site1	—
19	6.8	1985	0.45	Nahanni, Canada	Site2	—
20	6.9	1989	0.64	Loma Prieta	BRAN	UCSC
21	6.9	1989	0.51	Loma Prieta	Corralitos	CDMG
22	7	1992	1.43	Cape Mendocino	Cape Mendocino	CDMG
23	6.7	1994	0.73	Northridge-01	LA-Sepulveda VA	USGS/VA
24	6.7	1994	0.42	Northridge-01	Northridge-Saticoy	USC
25	7.5	1999	0.31	Kocaeli, Turkey	Yarimca	KOERI
26	7.6	1999	0.56	Chi-Chi, Taiwan	TCU067	CWB
27	7.6	1999	1.16	Chi-Chi, Taiwan	TCU084	CWB
28	7.9	2002	0.33	Denali, Alaska	TAPS pump sta. #10	CWB

ruins, and the calculation process is shown in Figure 12. The acceleration time history curve of PGA modulated to 0.06 g and 0.35 g after normalization in Tables 6, respectively, was input into the numerical model of building ruins, and the vertical displacement time history (mean value) of five monitoring points in Figure 11 was obtained, as shown in Figures 13 and 14.

Figure 13 shows that the average maximum vertical displacement $[D_{\max}]$ of the monitoring points of the life-saving passage is 28 mm and 70 mm under the action of the ground motion with PGAs of 0.06 g and 0.35 g in FEMA P695, and $[D_{\max}] \leq [D] = 72.5$ mm, which passes the safety evaluation. However, 48% of the ground motion will cause the secondary collapse of the life-saving passage when the PGA is 0.35 g, which is called the probability percentage of secondary collapse. Figure 14 shows that the $[D_{\max}]$ of the monitoring points of the life-saving passage is 31 mm and 71.6 mm under the action of the ground motion with PGAs of 0.06 g and 0.35 g in the Wenchuan aftershock, and $[D_{\max}] \leq [D] = 72.5$ mm, which passes the safety evaluation, and the probability of secondary collapse of the life-saving passage is 46%.

4. Safety Evaluation of the Life-Saving Passage under Aftershock after the Main Earthquake

The probability percentage of the secondary collapse of the life-saving passage under the action of aftershocks after the main earthquake can provide a reference for the rescue commanders at the earthquake site to quickly judge the safety of the life-saving passage. The probability percentage (P_i) of different aftershock magnitudes after different main earthquake magnitudes according to Table 3, under this conditional probability, the collapse possibility (P) of the life-saving passage can be calculated under the action of aftershocks. The magnitude range of the main earthquake is divided into 6.0–6.4, 6.5–6.9, 7.0–7.4, and ≥7.5. The rescue time section (aftershock effect time): 0–12 h, 12–24 h, 24–48 h, 48–72 h, 72–96 h, 96–120 h, 120–144 h, and 144–168 h. The probability percentage P of the secondary collapse of the life-saving passage in the 168 h rescue section under the aftershock effect after the main earthquake is shown in formula (6).

$$P = (P_1 \times P_1') + (P_2 \times P_2') + \ldots \ (P_i \times P_i') \ldots + (P_8 \times P_8'), \quad (6)$$

Table 5: 28 Wenchuan aftershock.

No.	Magnitude (Ms)	PGA (g)	Earthquake Name	Recording station	
				Station code	Station name
1	3.5	0.55	051AXY080514003703	Yongan, Anxian county	51AXY
2	3.6	0.48	051QCD080514012401	Qingchuan	51QCD
3	3.7	0.65	051AXY080514010102	Yongan, Anxian county	51AXY
4	3.8	0.49	051JYD080513102201	Jiangyou	51JYD
5	3.8	0.55	051LDL080513233002	Luding lengqi	51LDL
6	4	0.58	051LXM080514045001	Muka, Lixian county	51LXM
7	4.1	0.48	051JZW080512190402	Jiuzhai Wujiao	51JZW
8	4.2	0.61	051AXY080514090901	Yongan, Anxian county	51AXY
9	4.2	0.63	051SMC080514080803	Asbestos Wipe	51SMC
10	4.3	0.56	051LDD080725045402	Luding Detuo	51LDD
11	4.3	0.48	051JZW080531142202	Jiuzhai Wujiao	51JZW
12	4.4	0.58	051JYD080513133601	Jiangyou	51JYD
13	4.7	0.67	051SMX080609152802	Shimian xianfeng	51SMX
14	4.7	0.66	051JZW080528013502	Jiuzhai Wujiao	51JZW
15	4.7	0.47	051SMX080609152802	Shimian Xianfeng	51SMX
16	4.8	0.56	051LDD080513105901	Luding Detuo	51LDD
17	4.9	0.58	051LDL080517041601	Luding Lengqi	51LDL
18	5.1	0.46	051AXT080514172601	Tashui, Anxian county	51AXT
19	5.1	0.50	051HSL080512144102	Heishui Shuangliu	51HSL
20	5.2	0.66	051LDD080512214003	Luding Detuo	51LDD
21	5.3	0.56	051JZW080527160302	Jiuzhai Wujiao	51JZW
22	5.3	0.66	051JZG080527160302	Jiuzhai Guoyuan	51JZG
23	5.5	0.60	051LDS080512150101	Luding Lengqi	51LDL
24	5.7	0.66	051JZB080527163703	Jiuzhai Baihe	51JZB
25	5.8	0.62	051JZG080512145403	Jiuzhai Guoyuan	51JZG
26	6.1	0.58	051AXT080518010802	Diban, Anxian county	51AXT
27	6.3	0.77	051DYB080512144303	Deyang Baima	51DYB
28	6.4	0.76	051JZW080512144301	Jiuzhai Wujiao	51JZW

Table 6: PGA values corresponding to magnitudes (Boore [65] and Jiang [66]).

Magnitude (Ms)	4.0–4.4 M (g)	4.5–4.9 (g)	5.0–5.4 (g)	5.5–5.9 (g)	6.0–6.4 (g)	6.5~6.9 (g)	7.0–7.4 (g)	≥7.5 (g)
PGA	0.06	0.10	0.19	0.23	0.35	0.41	0.69	0.81

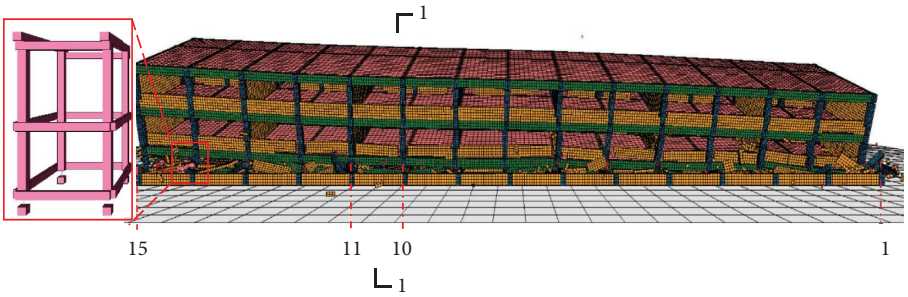

Figure 10: Overall numerical simulation model of collapsed ruins [51].

where P is the probability percentage of the secondary collapse of the life-saving passage in 12 h, 24 h, 48 h, and 72 h. P_i ($i = 1, \ldots, 8$) is the probability percentage of aftershocks of magnitudes 4.0–4.4, 4.5–4.9, 5.0–5.4, 5.5–5.9, 6.0–6.4, 6.4–6.9, 6.5–6.9, 7.0–7.4, and ≥7.5 within 168 h (as shown in Table 3). P_i' ($i = 1, \ldots, 8$) is the probability percentage of the secondary collapse of the life-saving passage under the action of the aftershocks of magnitude 4.0–4.4, 4.5–4.9, 5.0–5.4, 5.5–5.9, 6.0–6.4, 6.4–6.9, 7.0–7.4, and ≥7.5 within 168 h.

4.1. Safety Evaluation of Life-Saving Passage under FEMA P695 Ground Motion. The peak ground acceleration of the 28 ground motion records in FEMAP695 in Table 4 was modulated to 0.18 g, 0.22 g, 0.25 g, 0.41 g, 0.69 g, and 0.81 g when input into the numerical model of the life-saving passage, respectively. The vertical displacement time history of the life-saving passage monitoring points was calculated, as shown in Figure 15.

Figures 15(a)–15(f) show the vertical displacement time history of the key measuring points of life-saving passage

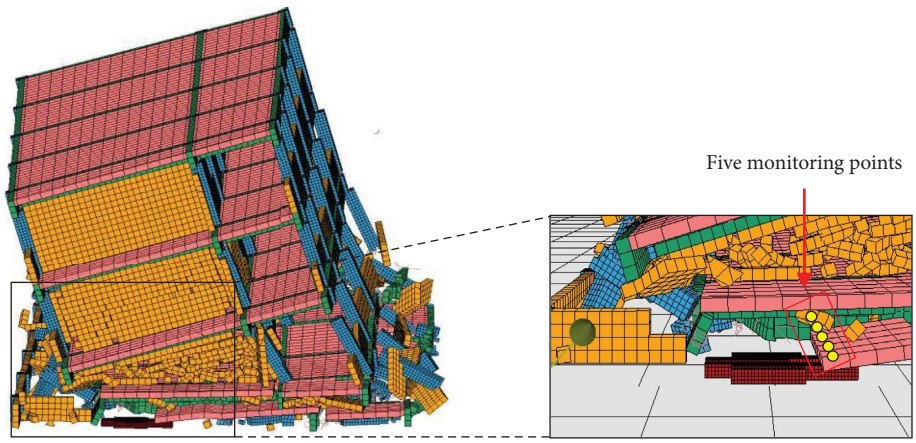

Figure 11: Section of the numerical simulation model of collapsed ruins [51].

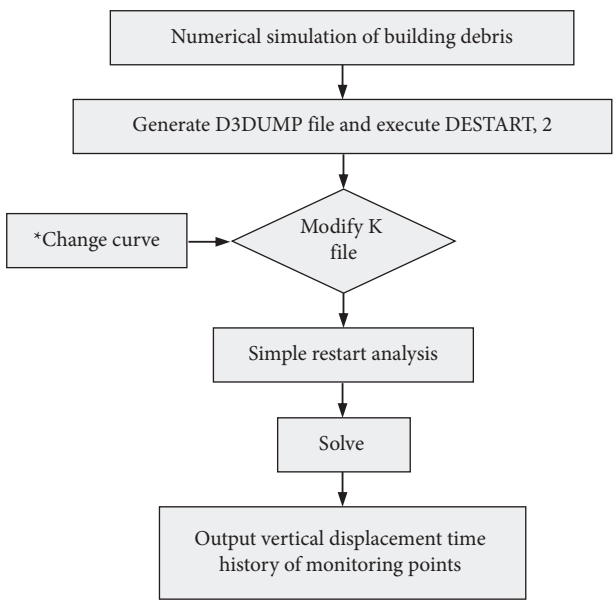

Figure 12: Restart calculation flow chart in LS-DYNA software.

includes steady descent (O-A), fast descent (A-B), and steady descent (C-D), accompanied by slight fluctuations under different PGA aftershocks, as shown in Figure 16. Additionally, there is a certain inflection point (A, B, and C) on the time history of vertical displacement curve. This inflection point can be used as an early warning point for secondary collapse of the life-saving passage under the action of aftershocks, which can refer to the literature on fire rescue and early warning [67–69]. The vertical displacement of the measuring points of life-saving passage increases nonlinearly with the increase of PGA value from 0.10 g to 0.81 g. The secondary collapse of the life-saving passage caused by different PGA aftershock is related to the rescue safety evaluation. However, it is usually difficult to predict the randomness of aftershocks after the main earthquake. Therefore, it is very valuable for the earthquake on-site rescuers to quickly evaluate the safety of the life-saving passage by considering the probability of aftershocks after the main earthquake. The probability percentage p' of the secondary collapse of the life-saving passage under the actions of different PGA aftershocks and the probability percentage p' of the secondary collapse of the life-saving passage is shown in Table 7.

The probability percentage (P) of the secondary collapse of the life-saving passage in rescue time of 0–12 h, 12–24 h, 24–48 h, 48–72 h, 72–96 h, 96–120 h, 120–144 h, and 144–168 h under the action of FEMA P695 ground motion are calculated when the magnitude of the main earthquake is 6.0–6.4, 6.5–6.9, 7.0–7.4, and ≥7.5, respectively, as shown in Table 8 and Figure 17.

The characteristics of the possibility of secondary collapse of the life-saving passage under ground motion in FEMA P695: the possibility of the secondary collapse of the life-saving passage increases with the increase of the magnitude of the main earthquake; the possibility of the secondary collapse of the life-saving passage increases exponentially with the increase of rescue time within "72-hour gold rescue," and the growth is slow after 72 hours when the magnitude of the main earthquake reaches above 7.4; the possibility of the secondary collapse of the life-saving passage increases linearly with the increase of rescue time when the magnitude of the main earthquake is 7.0–7.4; and the possibility of the secondary collapse increases slowly with the increase of the rescue time when the magnitude of the main earthquake is 6.0–6.9. The probability percentage (P) of the life-saving passage is between 3.87% and 8.27% when the magnitude of the main earthquake is 6.0–6.4; the P of the life-saving passage is between 6.12% and 10.58% when the magnitude of the main earthquake is 6.5–6.9; the P of the life-saving passage is between 17.58% and 37.71% when the magnitude of the main earthquake is 7.0–7.4; and the P of the life-saving passage is between 39.24% and 74.94% when the magnitude of the main earthquake is ≥7.4.

4.2. The Safety Evaluation of Life-Saving Passage under Wenchuan Aftershock. The peak ground acceleration of the 28 ground motion records in Wenchuan aftershock in Table 5 was modulated to 0.18 g, 0.22 g, 0.25 g, 0.41 g, 0.69 g, and 0.81 g when input into the numerical model of the life-saving passage, respectively. The vertical displacement time

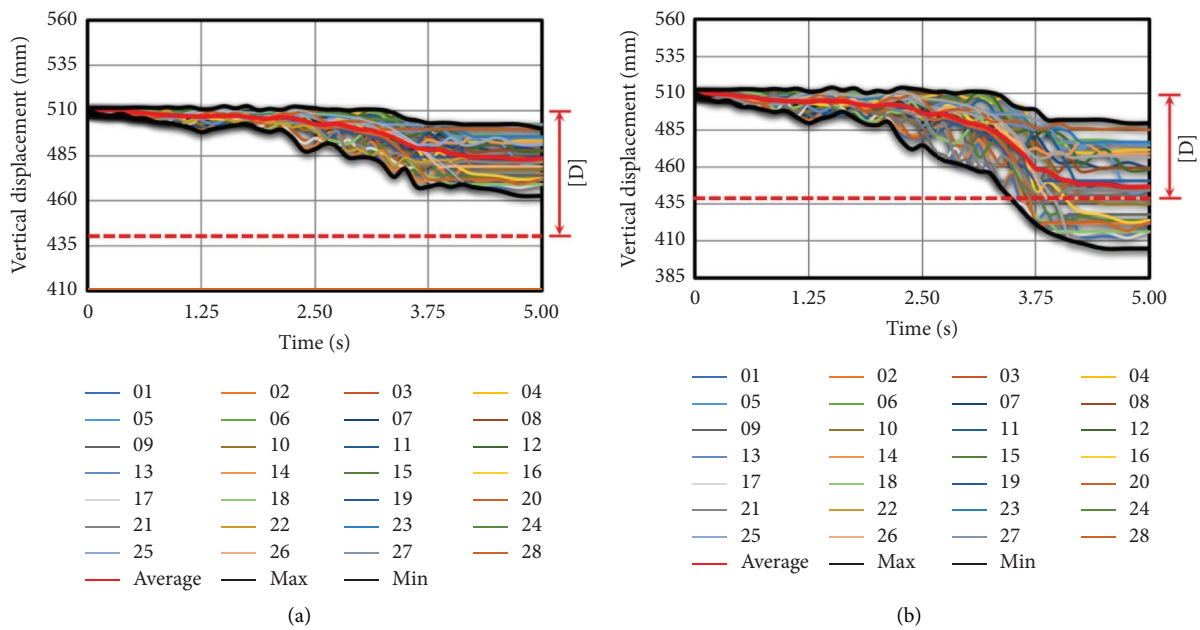

Figure 13: The vertical displacement time history of monitoring points under 28 ground motion (FEMA P695). (a) PGA 0.06 g. (b) PGA 0.35 g.

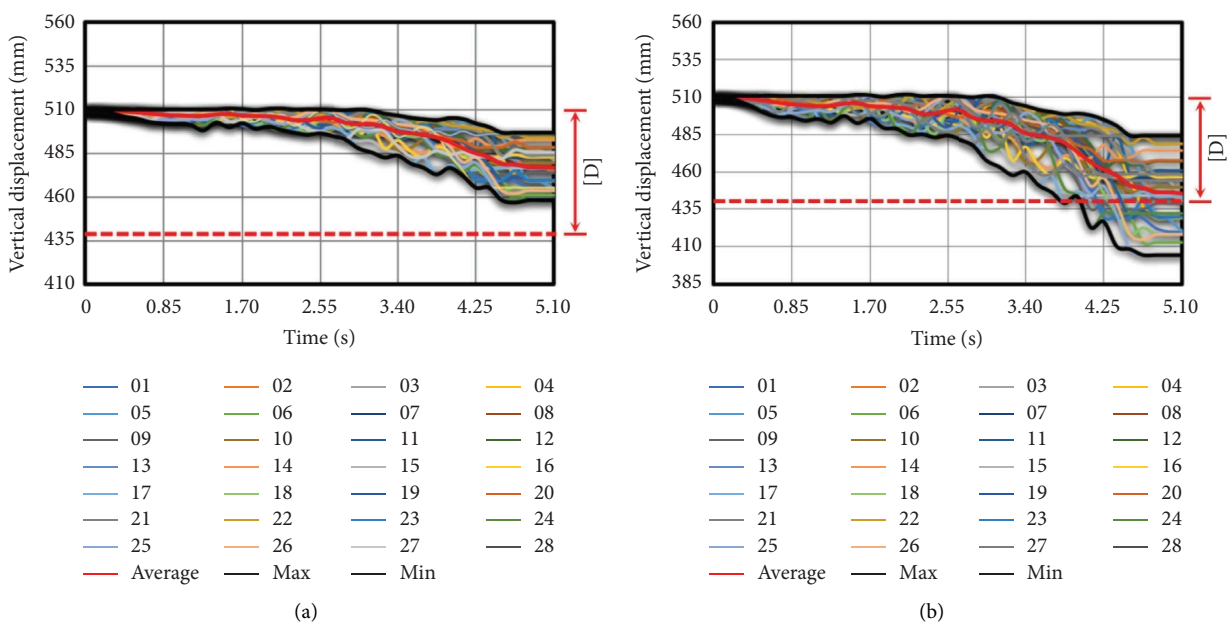

Figure 14: Vertical displacement time history of monitoring points under 28 ground motions (Wenchuan aftershocks). (a) PGA 0.06 g. (b) PGA 0.35 g.

history of the life-saving passage monitoring points was calculated, as shown in Figure 18.

Figure 18 is similar to Figure 15 in the vertical displacement time history of the key measuring points of life-saving passage, which is not to be repeated. Figure 18 shows the probability percentage p' of the secondary collapse of the life-saving passage under the actions of different PGA aftershocks and the probability percentage p' of the secondary collapse of the life-saving passage, as shown in Table 9.

The probability percentage (P) of the secondary collapse of the life-saving passage in rescue time of 0–12 h, 12–24 h, 24–48 h, 48–72 h, 72–96 h, 96–120 h, 120–144 h, and 144–168 h under the action of FEMA P695 ground motion are calculated when the magnitude of main earthquake is 6.0–6.4, 6.5–6.9, 7.0–7.4, and ≥7.5, respectively, as shown in Table 10 and Figure 19.

The characteristics of the possibility of secondary collapse of the life-saving passage under ground motion in

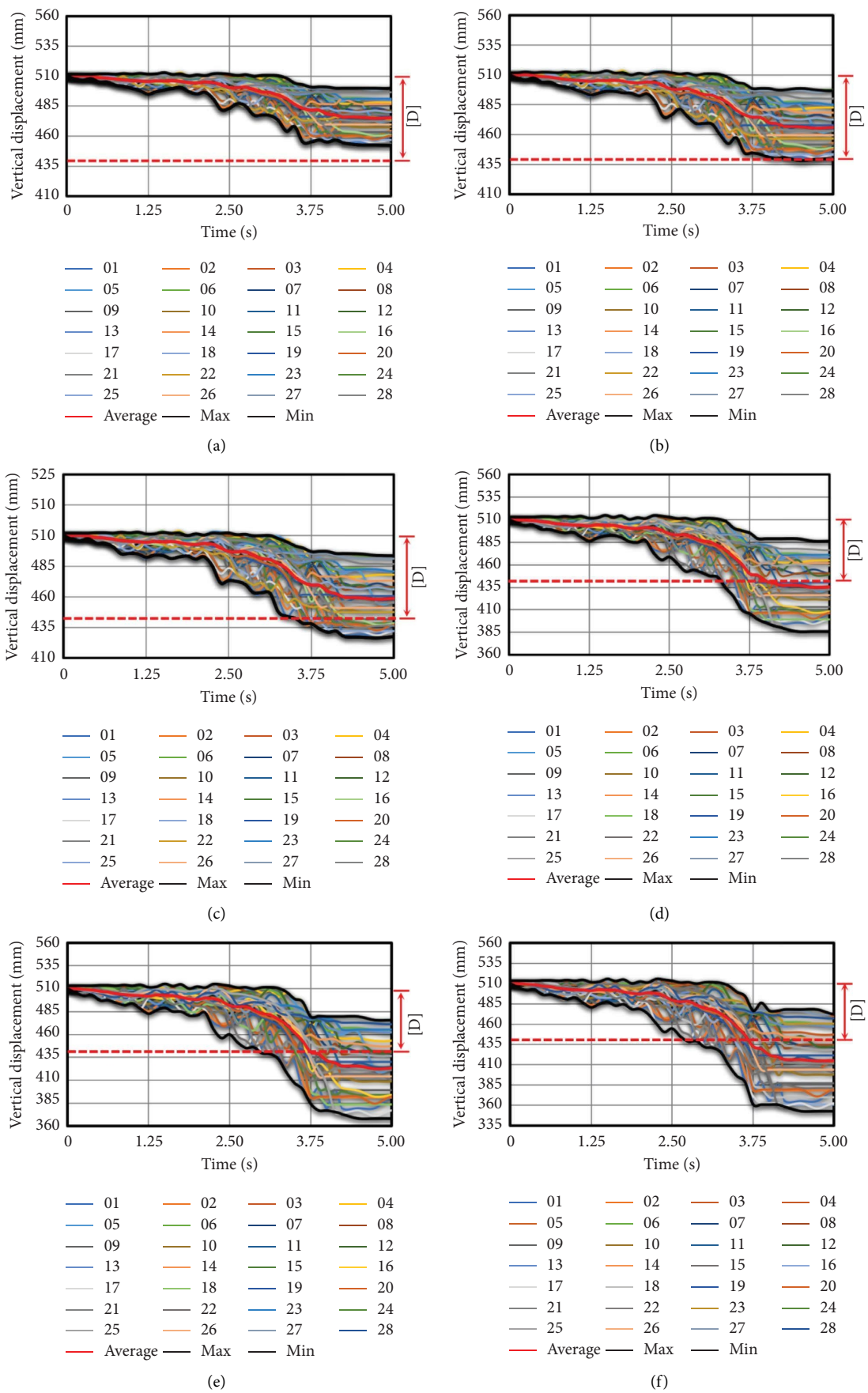

Figure 15: The vertical displacement time history of monitoring points under 28 ground motions (FEMA P695). (a) PGA 0.10 g. (b) PGA 0.19 g. (c) PGA 0.23 g. (d) PGA 0.41 g. (e) PGA 0.69 g. (f) PGA 0.81 g.

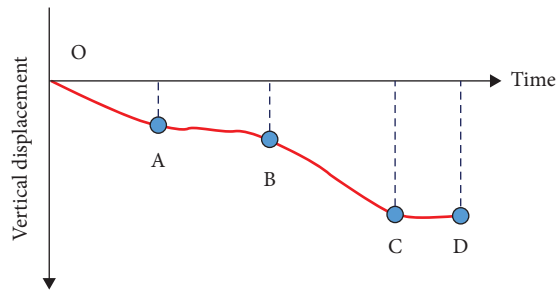

Figure 16: Schematic diagram of vertical displacement variation.

Table 7: The probability percentage p' (%) of the secondary collapse of the life-saving passage.

Aftershock	4.0–4.4	4.5–4.9	5.0–5.4	5.5–5.9	6.0–6.4	6.5–6.9	7.0–7.4	≥7.5
P'	0	0	7.14	21.4	35.7	42.8	71.4	82.1

Table 8: The probability percentage P (%) of the secondary collapse of the life-saving passage under aftershock after the main earthquake within 168 h rescue time.

Main earthquake magnitude	Rescue time							
	≤12 H	≤24 H	≤48 H	≤72 H	≤96 H	≤120 H	≤144 H	≤168 H
6.0–6.4	3.87	5.08	6.53	6.98	6.98	7.66	7.81	8.27
6.5–6.9	6.12	7.99	8.66	9.17	10.32	10.32	10.58	10.58
7.0–7.4	17.58	17.58	23.45	28.79	29.81	29.81	32.87	37.71
≥7.5	39.24	60.15	64.73	74.94	74.94	74.94	74.94	74.94

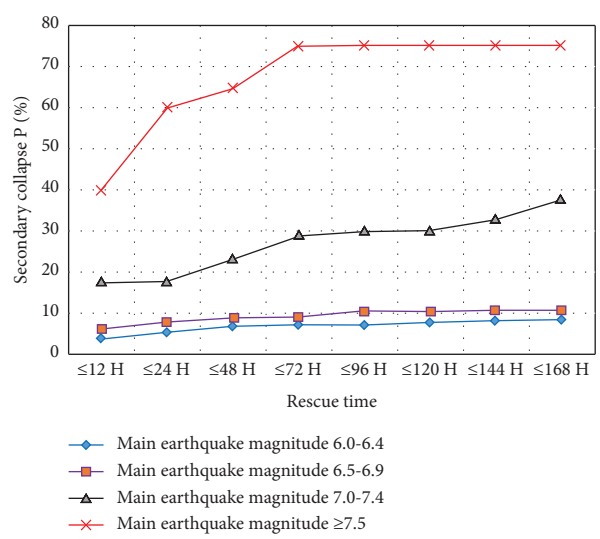

Figure 17: The probability percentage P (%) of the secondary collapse of the life-saving passage under aftershock after the main earthquake within 168 h rescue time.

Wenchuan aftershocks: the possibility of the secondary collapse of the life-saving passage increases with the increase of the magnitude of the main earthquake; the possibility of the secondary collapse of the life-saving passage increases exponentially with the increase of rescue time within "72-hour gold rescue," and the growth is slow after 72 hours when the magnitude of the main earthquake reaches above 7.4; the possibility of the secondary collapse of the life-saving passage increases linearly with the increase of rescue time when the magnitude of the main earthquake is 7.0–7.4; and the possibility of the secondary collapse increases slowly with the increase of the rescue time when the magnitude of the main earthquake is 6.0–6.9. The probability percentage (P) of the life-saving passage is between 4.85% and 9.79% when the magnitude of the main earthquake is 6.0–6.4; the P of the life-saving passage is between 6.88% and 12.35% when the magnitude of the main earthquake is 6.5–6.9; the P of the life-saving passage is between 21.14% and 44.85% when the

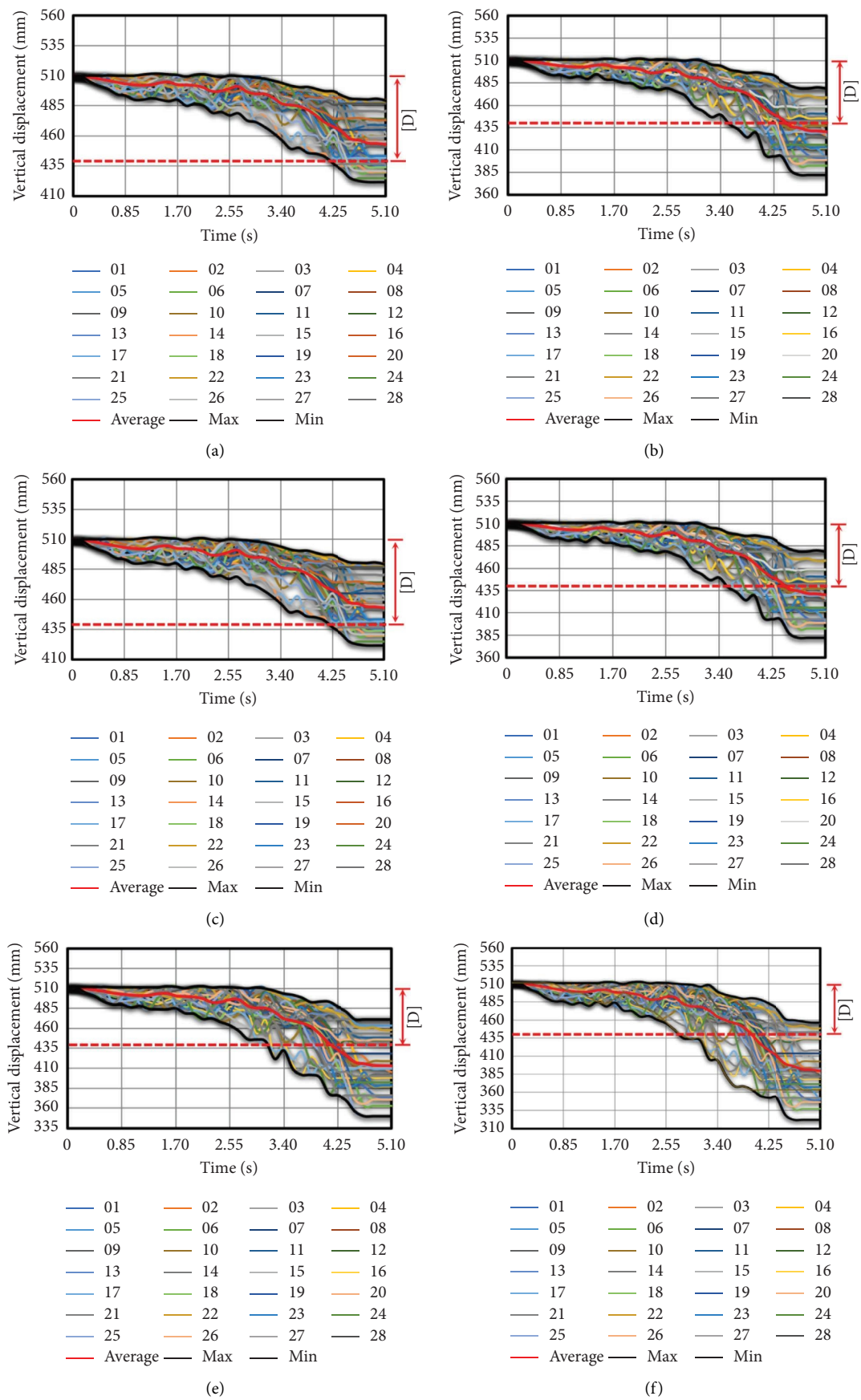

Figure 18: The vertical displacement time history of monitoring points under 28 ground motions (Wenchuan aftershocks). (a) PGA 0.10 g. (b) PGA 0.19 g. (c) PGA 0.23 g. (d) PGA 0.41 g. (e) PGA 0.69 g. (f) PGA 0.81 g.

Table 9: The probability percentage p' (%) of the secondary collapse of the life-saving passage.

Aftershock	4.0–4.4	4.5–4.9	5.0–5.4	5.5–5.9	6.0–6.4	6.5–6.9	7.0–7.4	≥7.5
p'	0	0	10.7	21.4	35.7	57.1	71.4	85.7

Table 10: The probability percentage P (%) of the secondary collapse of the life-saving passage under aftershocks after the main earthquake within 168 h rescue time.

Main earthquake magnitude	Rescue time							
	≤12 H	≤24 H	≤48 H	≤72 H	≤96 H	≤120 H	≤144 H	≤168 H
6.0–6.4	3.87	5.08	6.53	6.98	6.98	7.66	7.81	8.27
6.5–6.9	6.12	7.99	8.66	9.17	10.32	10.32	10.58	10.58
7.0–7.4	17.58	17.58	23.45	28.79	29.81	29.81	32.87	37.71
≥7.5	39.24	60.15	64.73	74.94	74.94	74.94	74.94	74.94

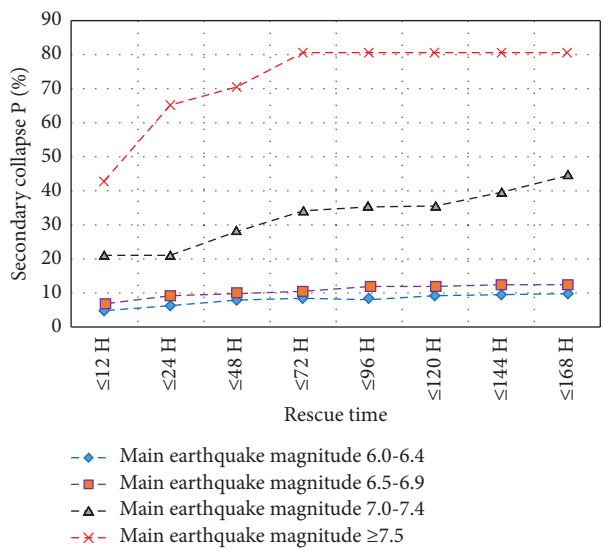

Figure 19: The probability percentage P (%) of the secondary collapse of the life-saving passage under aftershocks after the main earthquake within 168 h rescue time.

magnitude of the main earthquake is 7.0–7.4; and the P of the life-saving passage is between 42.83% and 80.56% when the magnitude of the main earthquake is ≥7.4.

Figures 16 and 18 are placed in the same coordinate system, as shown in Figure 20. The difference in the probability percentage (P) of the secondary collapse of the life-saving passage is within 5% under the action of FEMA P695 and Wenchuan aftershocks. The selection of aftershocks has a minimal impact on secondary collapse. The change trend in the probability percentage (P) of the secondary collapse is almost the same for the two kinds of earthquakes with the rescue time. The trend of the probability percentage (P) of the secondary collapse is mainly affected by the probability percentage (P_i) of different aftershock magnitudes after the main earthquake. The probability percentage (P) of the secondary collapse shows a linear growth trend in the rescue time section when the magnitude of the main earthquake is 7.0–7.4. The probability percentage (P) of the secondary collapse of the life-saving passage is almost unchanged when the magnitude of the main earthquake is ≥7.5 and after a 60-hour rescue time. It is recommended to refer to the safety factor K given in this paper if wood shoring is used to construct life-saving passages when the magnitude of the main earthquake is 6.0–7.4.

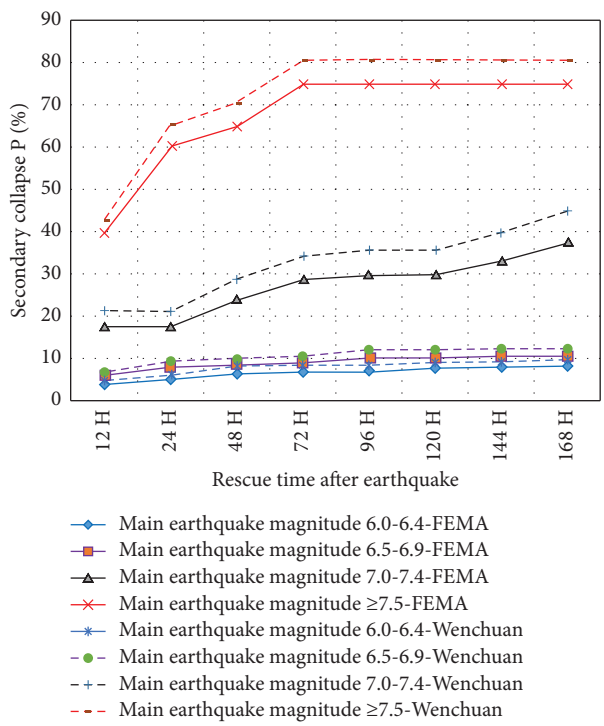

Figure 20: The probability percentage P (%) of the secondary collapse of the life-saving passage under aftershock after the main earthquake within 168 h rescue time.

It is also recommended to increase the safety factor K appropriately if wood shoring is used to construct life-saving passages when the magnitude of the main earthquake is ≥7.5.

5. Conclusions and Prospects

5.1. Conclusions. The safety evaluation method of saving-life passage in building ruins is studied in the rescue process. The safety evaluation indicator is proposed, which conforms to the construction characteristics of the building ruins and the life-saving passage. The method of safety evaluation of the life-saving passage in the building ruins is elaborated. The possibility of the second collapse of the life-saving passage is calculated under the aftershocks in different rescue time sections after the main earthquake. The main conclusions are as follows:

(1) Considering the characteristics of building ruins and the size of the living space of the trapped, the vertical displacement is proposed as an evaluation indicator of life-saving passage. Wood shoring is a necessary rescue technology to construct a life-saving passage in building ruins; therefore, the vertical displacement of wood shoring is considered the limit value of the safety evaluation indicator.

(2) The ultimate vertical deformation (D_{ultimate}) of the rescue wood shoring is obtained through the compression bearing capacity test. The allowable stress design is used to determine that the safety factor K of wood shoring is 2.5. The allowable vertical deformation $[D]$ value of life-saving passage is D_{ultimate} divided by 2.5. It is considered unsafe if the vertical deformation (D) of the life-saving passages exceeds $[D]$ under the actions of aftershocks.

(3) The selection of aftershocks has a minimal impact on secondary collapse of the life-saving passage. The change trend in the probability percentage (P) of the secondary collapse is almost the same for the two kinds of earthquakes with the rescue time. The trend of the probability percentage (P) of the secondary collapse is mainly affected by the probability percentage (P_i) of different aftershock magnitudes after the main earthquake.

(4) The probability percentage (P) of the secondary collapse shows a linear growth trend in the rescue time section when the magnitude of the main earthquake is 7.0–7.4. The probability percentage (P) of the secondary collapse of the life-saving passage is almost unchanged when the magnitude of the main earthquake is ≥7.5 and after a 60-hour rescue time.

(5) The possibility of the secondary collapse of the life-saving passage increases exponentially with the increase of rescue time within "72-hour gold rescue," and the growth is slow after 72 hours when the magnitude of the main earthquake reaches above 7.4; the possibility of the secondary collapse of the life-saving passage increases linearly with the increase of rescue time when the magnitude of the main earthquake is 7.0–7.4; and the possibility of the secondary collapse increases slowly with the increase of the rescue time when the magnitude of the main earthquake is 6.0–6.9.

(6) It is recommended to refer to the safety factor K given in this paper if wood shoring is used to construct life-saving passages when the magnitude of the main earthquake is 6.0–7.4. It is also recommended to increase the safety factor K appropriately if wood shoring is used to construct life-saving passages when the magnitude of the main earthquake is ≥7.5 during actual earthquake rescue process.

5.2. Prospects. The theoretical research on the safety evaluation of life-saving passage in building ruins under aftershocks is just at the beginning stage at home and abroad. This paper puts forward a research prospects for further study as follows:

(1) This paper proposes a method to evaluate the safety of life-saving passage in building ruins by the approach of numerical simulation, which can provide ideas for the follow-up research. Specially, the safety evaluation indicators need further investigation.

(2) This paper takes the pancake building ruins as the research object, actually, there are the incline-type building ruins, small space-type building ruins and V-type building ruins, and suspended-type building ruins in earthquake sites. The follow-up work can

focus on the safety evaluation of different types of building ruins under the action of aftershock.

(3) The influence of different ground motions on the secondary collapse of the life-saving passage in building ruins can be further investigated.

(4) Researchers can further study the change rule of the vertical displacement of the life-saving passage in building ruins under the aftershock, which can provide theoretical support for the early warning method for the secondary collapse of building ruins.

Data Availability

The data used to support the findings of this study are included within the article.

Disclosure

The funder had no role in the design of the study; in the collection, analyses, or interpretation of data; in the writing of the manuscript; or in the decision to publish the results.

Conflicts of Interest

The authors declare that they have no conflicts of interest.

Acknowledgments

The authors would like to thank the Key Laboratory of Earthquake Engineering and Engineering Vibration of China Earthquake Administration for convenient conditions to complete the shaking table test. This research was funded by the Key R&D projects of the Jilin Provincial Department of Science and Technology (nos. 20210203107SF, 20220202103NC, and 20230203043SF).

References

[1] B. Xu, *Research on Urban Disaster Prevention and Mitigation Planning*, Tongji University, Hanghai, China, 2007.

[2] M. Chen, *Research on Public Opinion Guidance of Government Response to Emergencies*, Huazhong University of science and technology, Wuhan, China, 2013.

[3] R. Z. Farahani, M. Lotfi, A. Baghaian, R. Ruiz, and S. Rezapour, "Mass casualty management in disaster scene: a systematic review of OR&MS research in humanitarian operations," *European Journal of Operational Research*, vol. 287, no. 3, pp. 787–819, 2020.

[4] D. Huang, S. Wang, and Z. Liu, "Humanitarian access interrupted: dynamic near real-time network analytics and mapping for reaching communities in disaster-affected countries," *Spectrum*, vol. 42, no. 3, pp. 815–834, 2021.

[5] Federal Emergency Management Agency, "Urban search and rescue response system," *Operations Manual in Federal Disaster Operations*, vol. 9356, pp. 589–607, 2000.

[6] S. Auclair, P. Gehl, and M. Delatre, "Needs and opportunities for seismic early warning prior to aftershocks for search and rescue teams: an in-depth analysis of practitioners' perceptions," *International Journal of Disaster Risk Reduction*, vol. 65, Article ID 102545, 2021.

[7] US Army Corps of Engineers, "Urban Search and Rescue," U. S. Army Corps of Engineers, Washington, DC, USA, Field Operation Guide, 2012.

[8] International search and Rescue Advisory Group, *INSARAG International Search and Rescue Guide*, International search and Rescue Advisory Group, Geneva, Switzerland, 2020.

[9] G. Liu, "Review and Reflection on the on-site rescue of the international rescue team," *City and disaster reduction*, vol. 02, pp. 7–12, 2019.

[10] International Seismological Centre, *Event 486403 Southern Greece. ISC Bulletin: Event Catalogue Search*, International Seismological Centre, Berkshire, UK, 2021.

[11] Y. T. Diamantis, *Kalamata Earthquake 1986: Ruins, terror and death*, Kalamata Earthquake, Beijing, China, 2022.

[12] L. R. Sheu, B. J. Shih, and C. W. Wu, "The search and rescue operation in collapsed buildings caused by earthquakes-a case study," in *Proceedings of the International Symposium on Automation and Robotics in Construction*, pp. 1–4, Taipei, Taiwan, January 2000.

[13] F. Zhize, "Analysis of typical rescue cases of wenchuan earthquake," *China Emergency Rescue*, vol. 41, no. 05, pp. 33–36, 2013.

[14] H. Murakami, T. Takemoto, and K. Sakamoto, "Study On Search And Rescue Operationsin The 1995 Hanshin-Awaji Earthquake–Analysis Of Labor Work In Relation With Building Types," in *Proceedings of the 12WCEE*, pp. 1–8, Auckland, New Zealand, February 2000.

[15] A. Koresawa, "Evidence-based analysis of search and rescue operations following the great east Japan earthquake," *Journal of Disaster Research*, vol. 8, no. sp, pp. 746–755, 2013.

[16] *66 Countries Send Help for Turkey Quake Victims*, 2011, https://www.msn.com/en-ph/news/national/66-countries-send-help-for-turkey-quake-victims-%e2%80%94-envoy/ar-AA17gCcQ.

[17] *The Weather Channel. Turkey Earthquake: Search and Rescue for Survivors*, 2023, https://weather.com/news/news/2023-02-17-turkey-earthquake-search-rescue-survivors.

[18] D. Wang, *Research on Earthquake Disaster Simulation and rescue Virtual Simulation Training System*, Institute of engineering mechanics, China Seismological Bureau, Beijing, China, 2009.

[19] H. Liu, *Preliminary Design and Implementation of Debris Safety Evaluation Expert System in Earthquake rescue*, Institute of engineering mechanics, China Earthquake Administration, Beijing, China, 2015.

[20] Abe books, *Appraisal Standard for Dangerous Building*, Abe books, Beijing, China, 2004.

[21] Abe books, *Earthquake Site Work Part II: Building Safety Appraisal*, Abe books, Beijing, China, 2001.

[22] D. Huang, S. Wang, and Z. Liu, "A systematic review of prediction methods for emergency management," *International Journal of Disaster Risk Reduction*, vol. 62, Article ID 102412, 2021.

[23] A. M. El-Maissi, S. A. Argyroudis, and F. M. Nazri, "Seismic vulnerability assessment methodologies for roadway assets and networks: a state-of-the-art review," *Sustainability*, vol. 13, no. 1, p. 61, 2020.

[24] Y. Li, "The collapsed building by earthquake: body searching and ruins cleaning-up," *Recent Developments in World Seismology*, vol. 05, pp. 31–36, 2012.

[25] W. Chen, Y. Wang, and J. Gu, *Earthquake Disaster Search and rescue Theory and method*, Earthquake Press, Beijing, China, 2008.

[26] E. Wang and B. Huang, *Earthquake Disaster Emergency Rescue Manual*, Earthquake Press, Beijing, China, 2008.
[27] F. E. M. A. Fema, *USAR Collapsed Building Technician Training Manual*, Federal Emergency Management Agency, Washington, DC, USA, 2011.
[28] L. Fan, C. Sun, and Y. Wang, "Research on the scene design of falling objects of debris structures in the simulation training of earthquake rescue in middle school teaching area," *Urbanism and Architecture*, vol. 16, pp. 118–123, 2017.
[29] L. Fan, *Research on Design Strategy of Earthquake rescue Simulation Training Ruins in Middle School Teaching Area*, Harbin University of Technology, Harbin, China, 2017.
[30] D. Xu, *Study on the Numerical Simulation of Earthquake Response Simulation of Buildings and Ruins Based on the Whole rescue process*, Institute of Engineering Mechanics, China Earthquake Administration, Beijing, China, 2022.
[31] D. Xu, J. Dai, Y. Yang, X. Weng, and G. Sun, "Study on numerical simulation of seismic collapse of RC frame structure with infilled wall," *Advances in Civil Engineering*, vol. 2022, Article ID 1890091, 24 pages, 2022.
[32] L. Guan, *Study on Rapid Assessment Method of Building Ruins Rescue Safety under Aftershock*, Institute of Engineering Mechanics, China Earthquake Administration, Beijing, China, 2022.
[33] C. Wu, *Numerical Simulation on Earthquake Collapse Process of Steel Frame Strucutre and Responses of its Ruins in Aftershocks*, Institute of Engineering Mechanics, China Earthquake Administration, Beijing, China, 2020.
[34] J. Hallquist, *LS-DYNA Eeoretical Manual*, Livermore Software Technology Corporation, Livermore, CA, USA, 1998.
[35] J. Ma and H. Tang, "Application of lateral timber shoring technology in collapsed buildings after earthquake," *China Emergency Rescue*, vol. 2021, no. 06, pp. 26–34, 2021.
[36] H. Tang and J. Ma, "Application of safety measures for rescue space in earthquake building collapse accident," *Shanxi Architecture*, vol. 48, no. 05, pp. 169–172, 2022.
[37] H. Tang and J. Ma, "Application of vertical wooden support technology in earthquake building collapse rescue," *China Emergency Rescue*, vol. 2021, no. 05, pp. 17–21, 2021.
[38] P. Jonn, *O'CONNEL, Emergency Rescue Shoring Techniques*, Pennwell Press, Tulsa, OK, USA, 2005.
[39] US Department Of Homeland Security, *Field Guide for Building Stabilization and Shoring Techniques*, US Department Of Homeland Security, Washington, DC, USA, 2011.
[40] S. Huang, H. Fang, D. Yu, R. Zheng, and Y. Chen, *A Fast rescue Shoring System with Angle and Pressure Monitoring and Alarm device*, China Earthquake Administration, Beijing, China, 2022.
[41] R. Allahabadi and G. H. Powell, "DRAIN-2DX user guide report UCB/EERC-88/06," *Earthquake Engineering Research Center University of California Berkeley*, vol. 6, 1988.
[42] H. Banon, J. M. Biggs, and H. M. Irvine, "Seismic damage in reinforced concrete frames," *Journal of the Structural Division*, vol. 107, no. 9, pp. 1713–1729, 1981.
[43] N. K. Gosain, R. H. Brown, and J. O. Jirsa, "Shear requirements for load reversals on RC members," *Journal of the Structural Division*, vol. 103, no. 7, pp. 1461–1476, 1977.
[44] Y. J. Park, A. H. S. Ang, and Y. K. Wen, "Seismic damage analysis of reinforced concrete buildings," *Journal of Structural Engineering*, vol. 111, no. 4, pp. 740–757, 1985.
[45] M. Roufaiel and C. Meyer, "Analytical modeling of hysteretic behavior of R/C frames," *Journal of Structural Engineering*, vol. 113, no. 3, pp. 429–444, 1987.
[46] TBI (Tall Buildings Initiative), *Guidelines for Performance-Based Seismic Design of Tall Buildings*, TBI (Tall Buildings Initiative), Berkeley, CA, USA, 2000.
[47] C. Architecture, *Code for Seismic Design of Building (GB50011-2010)*, China Architecture and Building Press, Beijing, China, 2010.
[48] Tsinghua University, *T/CECS 392-2021Design Standard for Collapse Resistance of Building structures*, Tsinghua University, China Academy of Building Sciences, Beijing, China, 2021.
[49] C. Nicola, "Monitoring, Prediction, and Early Warning Using Ground-Based Radar Interferometry," *Landslides*, vol. 7, pp. 291–301, 2010.
[50] F. Pratesi, T. Nolesini, S. Bianchini et al., "Early warning GBInSAR-based method for monitoring volterra (tuscany, Italy) city walls," *Ieee Journal of Selected Topics in Applied Earth Observations and Remote Sensing*, vol. 8, no. 4, pp. 1753–1762, 2015.
[51] J. P. O'Connell, "Supporting a fractured building," *Fire Engineering*, vol. 148, no. 11, pp. 64–71, 1995.
[52] China Architecture and Building Press, *Standard for Method Testing of Timber Structures*, China Architecture and Building Press, Beijing, China, 2012.
[53] NDS, *National Design Specification for Wood Construction*, American, Beijing, China, 2015.
[54] C. Earthquake Administration, *China Earthquake Examples*, Earthquake Press, Beijing, China, 2020.
[55] U.S. Department of the Interior, "Official Website of the U.S. Geological Survey," 2006, https://www.usa.gov.
[56] Y. Chen and D. C. Booth, "The Wenchuan earthquake of 2008: anatomy of a disaster, chapter 5: emergency response and rescue," *Translated World Seismology*, vol. 50, no. 01, pp. 79–99, 2019.
[57] H. Jian and M. A. Jian-fei, "Comparison of medical rescue efficiency between Wenchuan and Yushu earthquake disaster," *J Trauma Surg*, vol. 13, no. 05, pp. 431–433, 2011.
[58] X. Liu, R. Tong, and B. Li, "72 hours of non-stop rescue -- the rescue record of the National Mine Rescue Furong Team to the Ya'an earthquake disaster area," *Contemporary Miner*, vol. 6, p. 23, 2013.
[59] Xinhua News Agency reporter, "Feeling sad and highlighting strong-seven diaries of wenchuan earthquake," *Zhejiang Today*, vol. 361, no. 10, pp. 12–14, 2008.
[60] NetEase. Turkish FM: We support China's stance on COVID-19 [Video]. NetEase News. 2021, Retrieved from https://m.163.com/v/video/VESH5KBCV.html.
[61] https://www.bannedbook.org/ja/bnews/bannedvideo/20230213/1847811.html.
[62] Fema, *Quantification of Building Seismic Performance Factors*, FEMA, Washington, DC, USA, 2009.
[63] China Earthquake Networks Center, "Wenchuan aftershock sequences," 2017, http://www.ceic.ac.cn/history.
[64] D. M. Boore and G. M. Atkinson, "Ground-motion prediction equations for the average horizontal component of PGA, PGV, and 5%-damped PSA at spectral periods between 0.01sand 10.0s," *Earthquake Spectra*, vol. 24, no. 1, pp. 99–138, 2008.
[65] W. Jiang, *PGA Mixed Attenuation Relationship of Bedrock Site Based on Seismology*, Institute of Engineering Mechanics, China Earthquake Administration, Beijing, China, 2018.
[66] D. Xu, Y. Wang, D. Junwu, Y. Yongqiang, G. Liqian, and R. Agyare, "Study on numerical simulation method of seismic collapse of reinforce concrete frame structure," *Earthquake*

Engineering and Engineering Vibration, vol. 42, no. 3, pp. 134–142, 2022.

[67] J. wei, L. Guoqiang, and G. Lou, "Research on reliability of early-warning methods for collapse prediction of steel portal frames under fire," *Journal of Building Structures*, vol. 44, no. 02, pp. 164–174, 2023.

[68] L. Guoqiang, J. wei, C. Feng et al., "Collapse test of steel portal frame under fire and effective analysis of radar-based displacement measuring system," *China Civil Engineering Journal*, vol. 54, no. 09, pp. 56–65, 2021.

[69] L. Guoqiang, C. Feng, G. Lou, S. Jiang, and Y. Du, "Easy-measured key parameters and early-warning methods for the collapse prediction of steel portal frames under fire," *China Civil Engineering Journal*, vol. 54, no. 01, pp. 62–75+133, 2021.